Proc. Natl. Acad. Sci. USA
Vol. 94, pp. 9920–9925, September 1997
Neurobiology

Inactivation of the survival motor neuron gene, a candidate gene for human spinal muscular atrophy, leads to massive cell death in early mouse embryos

BERTOLD SCHRANK*, RUDOLF GÖTZ*, JENNIFER M. GUNNERSEN*, JANICE M. URE†, KLAUS V. TOYKA*, AUSTIN G. SMITH†, AND MICHAEL SENDTNER*

*Department of Neurology, University of Würzburg, 97080 Würzburg, Germany; and †Centre for Genome Research, University of Edinburgh, EH9 33Q Edinburgh, United Kingdom

Edited by Hans Thoenen, Max Planck Institute for Psychiatry, Martinsried, Germany, and approved June 23, 1997 (received for review May 5, 1997)

ABSTRACT **Proximal spinal muscular atrophy is an autosomal recessive human disease of spinal motor neurons leading to muscular weakness with onset predominantly in infancy and childhood. With an estimated heterozygote frequency of 1/40 it is the most common monogenic disorder lethal to infants; milder forms represent the second most common pediatric neuromuscular disorder. Two candidate genes—survival motor neuron (*SMN*) and neuronal apoptosis inhibitory protein have been identified on chromosome 5q13 by positional cloning. However, the functional impact of these genes and the mechanism leading to a degeneration of motor neurons remain to be defined. To analyze the role of the *SMN* gene product *in vivo* we generated *SMN*-deficient mice. In contrast to the human genome, which contains two copies, the mouse genome contains only one *SMN* gene. Mice with homozygous *SMN* disruption display massive cell death during early embryonic development, indicating that the *SMN* gene product is necessary for cellular survival and function.**

Proximal spinal muscular atrophy (SMA) is an autosomal recessive disorder characterized by loss of spinal motor neurons. The degeneration of these neurons leads to predominantly proximal symmetric muscle weakness and atrophy (1–3). Several types of the disease are distinguished by their time course and degree of motor function loss during postnatal development (4): In type I, the disease is manifest within the first 6 months of life; affected children generally die within the first 4 years of life. Type II patients show clinical weakness before 18 months and never stand or walk without support. Type III patients become symptomatic between 18 months and 30 years of life, with variable degrees of proximal weakness.

While this clinical classification system provides useful prognostic clues (5), molecular analysis has shown that both severe early onset and mild late onset forms are linked to the same chromosome locus 5q13 suggesting genetic homogeneity (6–9). Positional cloning strategies and deletion analysis have led to the identification of three candidate genes for spinal muscular atrophy, survival motor neuron *SMN* (10), neuronal apoptosis inhibitory protein *NAIP* (11), and transcript XS2G3 (12) [corresponding to exon 7 of the *NAIP* gene in reverse orientation (13)]. All these candidate genes are positioned within a complex region that is duplicated on the long arm of chromosome 5 (14), resulting in two copies of the *NAIP* and the *SMN* gene in the human genome. The *NAIP* gene shows homology to two baculovirus genes encoding inhibitor of apoptosis proteins (11). Its forced expression *in vitro* has been shown to suppress apoptosis in nonneuronal mammalian cells (15). *NAIP* exon 5 is deleted in 60% of type I SMA patients; in milder forms of the disease, deletions are identified only in 18% of affected individuals (11, 16–18). This gene is also deleted in 3% of normal carriers (11, 17), arguing that it is not essential for motor neuron survival or that its function can be compensated by other genes, in particular the truncated centromeric copy.

In contrast, 95% of SMA patients have deletions of the telomeric *SMN* gene regardless of phenotype severity (10, 16–20). This has led to the assumption that the *SMN* gene is the more likely candidate whose dysfunction is responsible for the disease (16–18). The two copies on chromosome 5q13, telomeric *SMN* copy (SMN^{tel}) and centromeric *SMN* copy (SMN^{centr}), differ only in five nucleotides in their coding regions, none of which causes an amino acid change. Rarely, asymptomatic carriers also show homozygous deletion of SMN^{tel} (16, 17, 20, 21). SMN^{centr} is deleted in 2–3% of normal carriers (10, 17–19). Four different small intragenic mutations have been identified in SMA patients that specifically disrupt SMN^{tel}, providing further evidence for the hypothesis that SMN^{tel} is the SMA disease-causing gene (10, 22). The centromeric gene copy (SMN^{centr}) is also expressed (10). However, developmental expression patterns and tissue distribution of these two isoforms have not been determined so far. Thus, it remains to be shown whether SMN^{centr} could compensate in case of the deletion of the telomeric copy or whether differential expression of both genes would not allow such functional overlap.

The *SMN* gene shows no homology to previously identified genes. Recently, a search for binding partners of the heterogeneous nuclear ribonucleoprotein U has identified *SMN* and subsequent immunohistochemical analysis revealed *SMN* localization in specific nuclear structures called gems (23). Based on the association of gems with coiled bodies a role of *SMN* in RNA metabolism has been suggested. Because the *SMN* gene is widely expressed both in neuronal and nonneuronal tissue (10), the specific degeneration of motor neurons, which is characteristic for spinal muscular atrophy, remains to be explained.

To characterize the role of the *SMN* gene during mammalian development we have identified the *SMN* homolog in the mouse and generated mice in which this gene is disrupted. In contrast to the human gene *SMN* is a single copy gene in the mouse. *SMN*-deficient mouse embryos develop normally until the compacted morula stage. Subsequent morphological alterations and degenerative changes lead to embryonic death

The publication costs of this article were defrayed in part by page charge payment. This article must therefore be hereby marked "*advertisement*" in accordance with 18 U.S.C. §1734 solely to indicate this fact.

This paper was submitted directly (Track II) to the *Proceedings* office.
Abbreviations: *SMN*, survival motor neuron; *NAIP*, neuronal apoptosis inhibitory protein; SMA, spinal muscular atrophy; SMN^{tel}, telomeric *SMN* copy; SMN^{centr}, centromeric *SMN* copy; p.c., post conception; ES, embryonic stem; E, embryonic day.
Data deposition: The sequence reported in this paper has been deposited in the GenBank database (accession no. Y12835).

prior to uterine implantation. The presence of degenerating, terminal deoxynucleotidyltransferase-mediated UTP end-labeling (TUNEL) positive cells in $SMN^{-/-}$ embryos demonstrates an essential role of the SMN protein for cellular survival and function and its potential involvement in regulatory processes underlying programmed cell death.

MATERIALS AND METHODS

Identification of the Mouse *SMN* Gene. A 527-bp PCR fragment corresponding to nucleotides 329–855 of human *SMN* (10) was used to screen a newborn mouse brain λZAP cDNA library (Stratagene) at low stringency. One candidate clone with an insert length of 1.3 kb (pSC4) contained an 891-bp ORF with high homology to the human *SMN* gene (exons 1–6). The C-terminal coding region corresponding to human exon 7 was identified by reverse transcription–PCR to be homologous as well. This region was separated from exon 6 by an unspliced intron of 106 bp in the pSC4 clone.

Generation of *SMN* Knockout Mice. Using pSC4 as a probe, two overlapping genomic clones, pSC6 and pSC7, were identified from a genomic library of 129/Ola-derived embryonic day (E) 14 embryonic stem (ES) cells, λPS (24). Using primers homologous to exons 1–6 of the human *SMN* gene in sequencing reactions, both clones were found to contain exons 2–4 and flanking intronic sequences. An 840-bp *Hin*dIII fragment of pSC7 containing the 5′ end of exon 2 was ligated into the *Xmn*I site of the targeting vector pGNA (25). The 3.8-kb *Hin*dIII/*Kpn*I fragment of pSC7 was then introduced into the *Sma*I/*Kpn*I site of pGNA. The *Kpn*I linearized targeting construct was electroporated into E14Tg2a-IV ES cells, grown without feeders and selected in the presence of G418 as described (26).

Homologous integration events were screened for by PCR and confirmed by restriction analysis of both 5′ (probe a) and 3′ ends (probe b) (Fig. 1*b*). Probe a was a 500-bp *Bam*HI/*Hin*dIII fragment upstream of the targeting construct, probe b was a 330-bp fragment (aa 65–174) amplified by PCR from pSC4. Five of 125 ES cell clones showed homologous integration events. Two clones injected into C57BL/6 blastocysts gave rise to germ-line transmission of the mutated allele. Chimeras were mated with outbred MF1 albino females. Heterozygous offspring were backcrossed to the MF1 strain. Intercross progeny were generated at the N1 and N2 generations. Progeny and E12 embryos were genotyped by Southern hybridization of mouse tail DNA *Bam*HI digests using probe a.

Analysis of Embryos. Following superovulation and mating of $SMN^{+/-}$ female mice with $SMN^{+/-}$ males the animals were sacrificed approximately 56 hr after mating and early morulae were obtained by tearing the oviducts. Each embryo was subsequently transferred to a drop of M16 medium overlaid with mineral oil and incubated at 37°C and 5% CO_2/95% air. Under these conditions (27), wild-type embryos could be maintained for 5 days without morphological evidence of degeneration (data not shown).

Embryos were photographed after 24 and 36–48 hr of culture before they were harvested for DNA analysis. Each embryo was transferred into a PCR tube containing 10 μl of PCR lysis buffer (50 mM KCl/10 mM Tris, pH 8.3/2.5 mM $MgCl_2$/0.1 mg/ml gelatin/0.45% Nonidet P-40/0.45% Tween 20/200 μg/ml Proteinase K) and incubated at 55°C for 1 hr and at 95°C for 15 min. Amplification of the mutant allele was performed with the primer pair used for the ES cell screen (forward 5′-CGTCTTATGGTATGGCAACTG-3′, reverse 5′-CATGCTGGGTACATGAAAACC-3′), amplification of the wild-type allele with a primer pair spanning the insertion site (sense 5′-GATGATTCTGACATTTGGGATG-3′, antisense 5′-TGTTTCAAGGGAGTTGTGGC-3′). PCR conditions were: a 1-min 95°C heating step, followed by 30 cycles of 95°C for 30 sec, 56°C for 1 min, 72°C for 90 sec, and a final 10 min incubation at 72°C. Samples were run on 2% agarose gels, blotted, and hybridized according to standard methods (28).

TUNEL Staining. Embryos derived from $SMN^{+/-}$ intercrosses were washed with PBS and fixed in 4% paraformaldehyde/PBS for 5 min at room temperature. They were subsequently washed three times with PBS for 5 min and permeabilized in 0.1% Triton X-100/0.1% sodium citrate for 2 min on ice. Following two rinses with PBS they were incubated with terminal deoxynucleotidyl transferase and fluorescein-labeled dUTP (In Situ Cell Death Detection Kit, Boehringer Mannheim) at 37°C for 1 hr. Embryos were subsequently destained three times with PBS for 10–15 min before they were analyzed and photographed under the fluorescence microscope. Except for the labeling mix, 1% FCS was added to all solutions to prevent the fragile embryos from sticking to the surface of the plastic dishes. After analysis, the embryos were individually transferred into PCR tubes and processed for genotyping as described previously. To increase the sensitivity of this analysis, a multiplex PCR assay was applied using a common forward primer (5′-CTCCGGGATATTGGGATTG-3′) and two reverse primers specific for the wild-type (5′-GTTGTGGCATTCTTCTGGC-3′) and mutant (5′-GGTAACGCCAGGGTTTTCC-3′) *SMN* genes. PCR conditions were identical with those described above. This methodological change allowed us to increase the number of embryos that could be genotyped after TUNEL staining. Five embryos from three litters could thus be identified as homozygous mutants and all of them showed strong TUNEL staining as shown in Fig. 2*k*.

***LacZ* Expression.** Whole-mount embryos were fixed in 2% paraformaldehyde/0.2% glutaraldehyde/PBS for 5 min, washed three times with PBS, and stained overnight at 37°C in 1 mg/ml 4-Cl-5-Br-3-indolyl-β-galactoside [4% 5-bromo-4-chloro-3-indolyl β-D-galactoside (X-Gal) dimethylsulfoxide stock solution], 5 mM potassium ferricyanide, 5 mM potassium ferrocyanide, 2 mM $MgCl_2$ in PBS as described (29). Ovaries were immersion-fixed with 2% paraformaldehyde for 30 min, washed briefly with PBS, and cryoprotected in 30% sucrose/PBS overnight. The tissue was embedded in Tissue-Tek (Miles), frozen by immersion in isopentane, and mounted on gelatine-coated slides after cryostat sectioning. Following a brief rinse in PBS, sections were fixed with 0.2% glutaraldehyde, 5 mM EGTA, 2 mM $MgCl_2$/PBS for 5 min, rinsed briefly, and stained with the X-Gal solution (see above) at 30°C overnight. After a rinse in PBS these sections were counterstained for 1 min with 1% neutral red in 50 mM sodium acetate buffer (pH 3.3) before dehydration in 70%, 90%, and 96% ethanol (modified from ref. 27).

Histological Analysis of Facial Motoneurons. Five-month-old $SMN^{+/+}$ and $SMN^{+/-}$ mice were perfused with 4% paraformaldehyde, and the brainstem regions containing the facial nuclei were dissected and processed as described (30). Briefly, paraffin serial sections (7 μm) were prepared and stained with cresyl violet. Only those facial motoneurons that showed a clearly detectable nucleus and nucleolus were counted in every fifth section. The motoneuron counts were corrected for double counting of split nucleoli, applying the formula introduced by Abercrombie as described (30).

RESULTS AND DISCUSSION

Cloning and Gene Targeting of the Mouse *SMN* Gene. As a first step in our analysis, a mouse *SMN* cDNA clone was identified from a newborn mouse brain cDNA library by low stringency hybridization using a probe corresponding to nucleotides 329–855 of the human *SMN* cDNA sequence (10). The predicted mouse *SMN* protein shares 83% amino acid identity with the human protein (Fig. 1*a*). Northern blot analysis indicates that *SMN* mRNA is widely expressed (data not shown), which corresponds to the expression of *SMN*

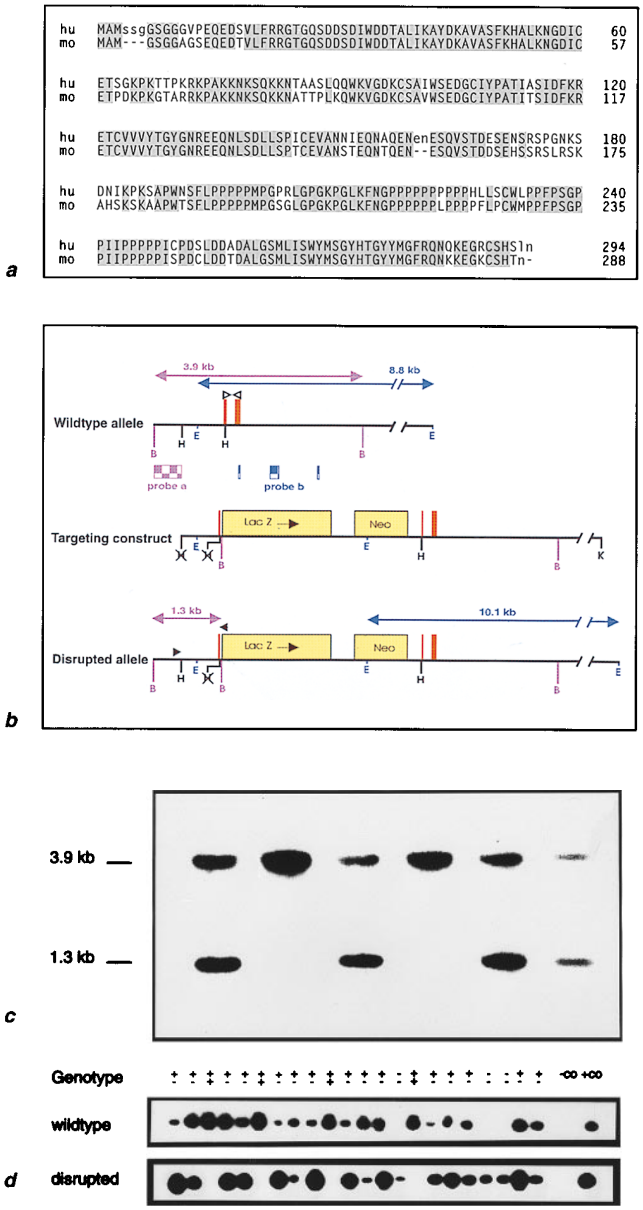

FIG. 1. Disruption of the murine *SMN* gene. (*a*) Amino acid sequence of the human (10) and mouse SMN protein. Uppercase letters represent related residues, shaded boxes highlight identities. The protein appears highly conserved with 83% identical and 98% related residues (31). The largest uninterrupted region of complete identity is found near the amino terminus with 46 aa. The characteristic proline-rich region from aa 190–246 (54% proline content) is also preserved. The expected M_r is 31.2 kDa. (*b*) Targeted disruption of the *SMN* gene. Partial genomic structure of the mouse *SMN* locus. Sizes of diagnostic restriction fragments are shown as arrows (purple, 5′ end; blue, 3′ end). Tiled boxes represent the DNA probes used for confirmation of targeting events. Solid triangles indicate primer position for the PCR screen of the mutated locus, open triangles indicate primer position for amplification of DNA corresponding to the wild-type allele. The relative position of exon 2 is shown by red bars. While splice junctions in the coding region are generally preserved between human and mouse, exon 2 of the mouse gene is fragmented by a small 200 bp intron. The *Hin*dIII site in exon 2 (aa 38 and 39) was used to disrupt the gene by insertion of the targeting vector pGNA (25) providing an in-frame *lacZ* fusion and the *neo*^{r} gene under a separate promoter. Genes supplied by pGNA are shown as yellow boxes (not drawn to scale). B, *Bam*HI; H, *Hin*dIII; E, *Eco*RI; K, *Kpn*I. (*c*) Genotyping of heterozygous intercross progeny: Densitometric analysis of signal intensities of bands corresponding to mutated and wild-type alleles revealed a ratio of 1.1 ± 0.15 (SD, $n = 11$). This confirms that the *SMN* gene is not duplicated in mice. (*d*) PCR genotyping of blastocyst stage embryos. The wild-type allele was identified with primers corresponding to the 5′ and 3′ end of exon 2 (*Upper*). Primers shown in *b* were used to amplify the mutant allele (*Lower*).

mRNA in human (10). In contrast to multiple transcripts of the human *SMN* genes originating from alternative splicing of exons 5 and 7 (10, 32), no evidence for alternative splicing in the mouse *SMN* sequence corresponding to the C-terminal part of the SMN protein was obtained. reverse transcription–PCR analysis of exons 4–8 revealed only a single amplification product from RNA derived from mouse embryonic stem cells, primary embryonic fibroblasts, brain, spinal cord, muscle, spleen, kidney, and testes (data not shown).

Restriction analysis of genomic mouse DNA indicated that the mouse genome contains only one copy of the *SMN* gene. This observation was corroborated by Southern blot analysis of ES cells after homologous recombination (see below). We designed a targeting vector in which the *Escherichia coli lacZ* gene is fused in-frame to the first 40 nucleotides of exon 2. A neomycin resistance gene under a separate promoter is positioned 3′ to the *lacZ* sequence (Fig. 1*b*). Homologous integration into the *SMN* locus in five independent ES cell clones was verified by Southern blot hybridization. The 1:1 ratio of signal intensity of bands corresponding to mutant and wild-type *SMN* in all five ES cell lines confirmed that *SMN* in the mouse is a single copy gene (data not shown). Two independent lines of heterozygous mice were generated following blastocyst injection.

Intercrosses of heterozygotes from both lines failed to produce homozygous $SMN^{-/-}$ progeny. Analysis of E12 embryos from heterozygous intercrosses also did not show any $SMN^{-/-}$ progeny (Table 1). Heterozygous intercrosses segregated $SMN^{+/-}$ and $SMN^{+/+}$ in a 2:1 ratio, indicating that homozygous *SMN* disruption results in an early lethal phenotype (Fig. 1*c*). There was no indication of increased uterine resorption, suggesting that $SMN^{-/-}$ embryos do not implant.

Massive Cell Death in Early $SMN^{-/-}$Embryos. Progeny from heterozygous intercrosses were isolated as uncompacted 5–7 cell morulae 56 hr p.c. The embryos were maintained in culture for 2–2.5 days and subsequently genotyped by PCR (Fig. 1*d*). During this time period, normal morulae first compact (8–16 cell stage) and then differentiate to blastocysts with the formation of an inner cell mass and the outer trophoblast cells (33). Homozygous mutant embryos initially were indistinguishable from wild-type and heterozygous embryos. At approximately 80 hr p.c., however, mutant embryos showed signs of aberrant development. Although morula compaction proceeded in most mutant embryos (Fig. 2*f*), the spherical shape of the embryos was subsequently lost and they appeared shrunken. In contrast to control embryos (Fig. 2 *a–d*), mutant embryos failed to form a blastocoel cavity. At later time points the embryos decompacted (Fig. 2*g*) and became progressively more disorganized and fragmented, often with bleb-like protuberances (Fig. 2*h*). At 90–100 hr p.c., extensive cellular degeneration occurred in all mutant embryos (Fig. 2*i*). TUNEL staining of such embryos revealed a high number of intensely labeled cells indicative of apoptotic cell death (Fig. 2*k*). In contrast, heterozygous and wild-type blastocysts only revealed very few apoptotic cells (34) (Fig. 2*e*). These experiments confirmed that homozygous *SMN* disruption in the mouse leads to developmental arrest and death prior to implantation (Table 1).

SMN mRNA is highly expressed in oocytes in the ovary of adult mice as shown by *lacZ* expression (Fig. 3*a*). This would indicate that the SMN protein is made in oocytes of mothers with an intact gene copy and may be transferred to and used by early embryonic cells during the first rounds of division. The persistence of maternally produced SMN protein in the em-

Table 1. $SMN^{+/-}$ intercross progeny

		Genotype				
		+/+	+/−	−/−	Untyped	Total
Live born		10	25	0		35
E12		8	16	0		24
	Total	18	41	0		59
Preimplantation	Exp. 1	4	15	3	2	24
	Exp. 2	6	15	9	5	35
	Exp. 3	2	5	3	1	11
	Exp. 4	10	14	3	0	27
	Total	22	49	18	8	97
Phenotype						
Blastocyst		16	43	1	3	63
Morula arrest		3	4	15	1	23
Abnormal cleavage stage		3	2	2	4	11

Routine genotyping was performed by Southern blot hybridization of mouse tail genomic DNA. Genotype–phenotype correlation of early embryonic progeny. The mid-portion of the table shows the genotype of embryos observed in four independent experiments (N2 progeny intercrosses). Embryos at the early morula stage [56–60 hr post conception (p.c.) in experiments 1, 2, 4, 46 hr p.c. in experiment 3] were recovered from the oviduct and kept in culture until the full blastocyst stage had developed (100–110 hr p.c.). Genotyping was performed by PCR analysis of individual embryos. Segregation of wild-type, hetero- and homozygous mutant genotypes observed does not differ significantly from a Mendelian pattern ($\chi^2 = 0.703$; df 2; $P = 0.70$). The lower portion of the table shows the respective phenotypes: Blastocysts, normal development with formation of the inner cell mass and a thin walled trophoblast; Morula arrest, normal early morula (5–8 cells), but failure to progress to the blastocyst stage (Fig. 2); Abnormal cleavage stage embryos, abnormal on isolation, often with degenerating cells. Such embryos are commonly found in laboratory mice, particularly following superovulation. No significant difference was found in the number of abnormal cleavage stage embryos between homozygous mutant and heterozygous/wild-type embryos ($\chi^2 = 0.33$; df 1; $P = 0.57$). This indicates that embryonic lethality at premorula stages is not specifically associated with the *SMN* phenotype. The association of the morula arrest phenotype with a homozygous mutant genotype is highly significant ($\chi^2 = 45.35$; df 1; $P < 0.0001$).

bryo could explain the normal development of *SMN* deleted embryos to the early morula stage despite deletion of the *SMN* gene in the embryo. Embryonic expression of *SMN* became appreciable at the late morula stage as assessed by detection of β-galactosidase activity in embryos generated by mating heterozygous males with wild-type females (Fig. 3 *b* and *c*). Thus, the death of mutant embryos may coincide with depletion of maternal *SMN* in these embryos.

Implications of the Murine $SMN^{-/-}$ Phenotype for Human SMA. These results show that complete loss of *SMN* in the mouse leads to massive cell death during early embryonic development. The striking difference between the phenotype

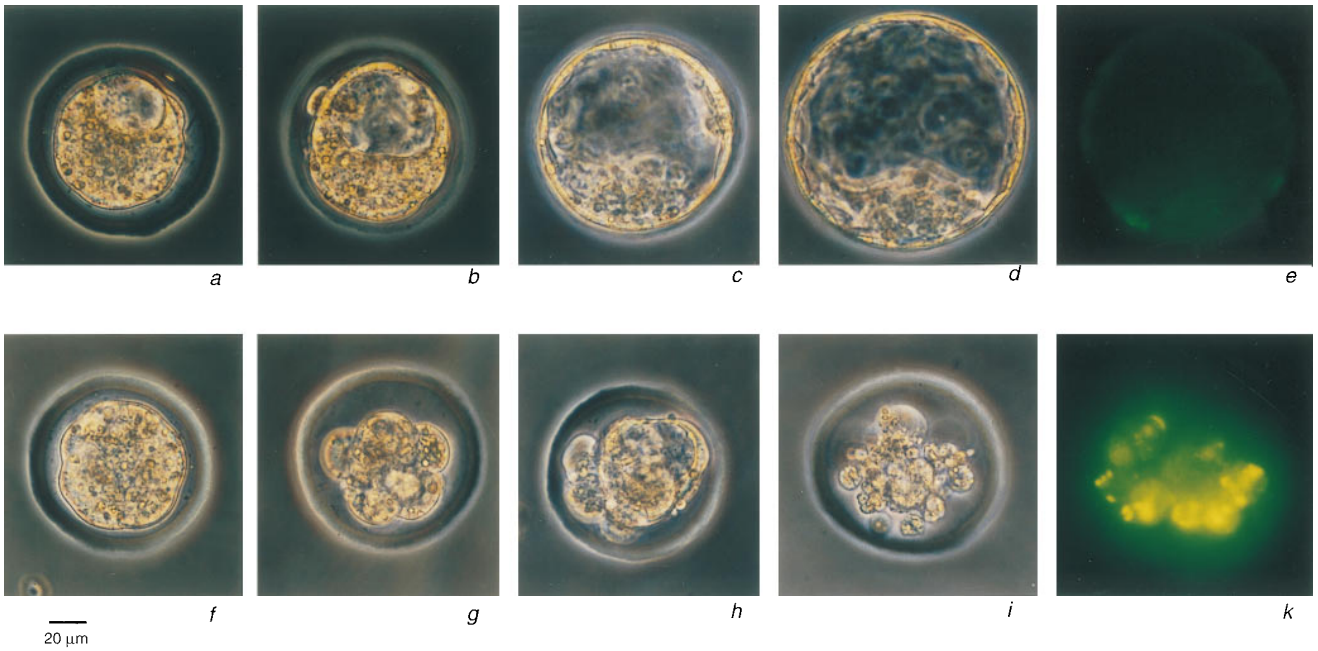

FIG. 2. Morphological alterations and TUNEL staining in control and mutant *SMN* embryos. (*a–e*) Wild-type or heterozygous embryos. (*f–k*) Homozygous mutant embryos at equivalent time points. A failure in transition to the blastocyst stage first became apparent at 80–90 hr after mating (*g* and *h*), with subsequent formation of a disorganized, multicystic structure (*h*) and finally extensive cellular degeneration (*i*) at 90–104 hr p.c. TUNEL staining of $SMN^{-/-}$ embryos showed strong staining of most cells, suggesting apoptotic cell death (*k*). In contrast, wild-type blastocysts showed only very few labeled cells (*e*).

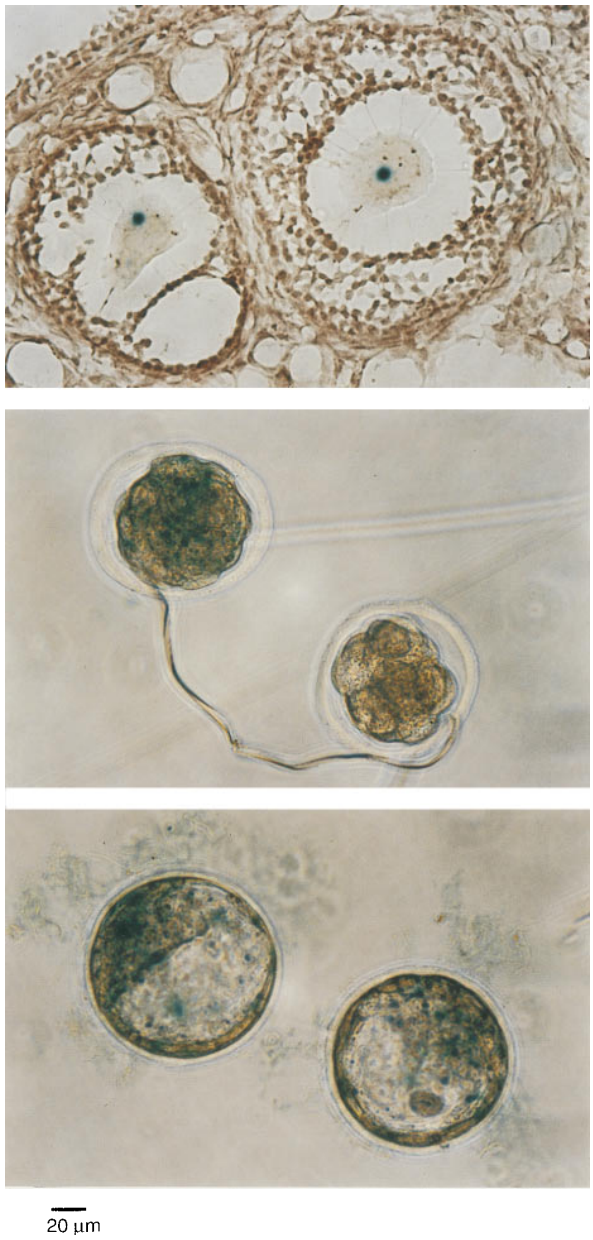

FIG. 3. *SMN*$^{+/-}$ *lacZ* Expression. (*a*) Strong expression was found in oocytes of pregnant mare serum gonadotrophin-treated female heterozygotes. (*b* and *c*) Embryo *lacZ* expression. Heterozygous males were mated to wild-type females to determine the onset of embryonic *SMN* expression. Whereas 5–8 cell morulae did not show any staining (*b Right*), compacted morulae (8–16 cells) expressed the reporter gene (*b Left*). β-Galactosidase activity was apparent in both inner cell mass and trophoblast cells at the blastocyst stage (*c*).

resulting from loss of the *SMN* gene in mouse and human could be explained by gene copy number: the mouse genome contains only a single *SMN* gene copy, whereas the human genome contains two copies at the same locus with nearly identical coding sequence. Both human copies are expressed (10). Loss of the centromeric copy of the gene is not associated with a recognizable phenotype (10, 17–19). Genetic data, in particular the identification of healthy individuals with homozygous deletion of the telomeric copy (16, 17, 20, 21), suggest functional redundancy in humans. Although full compensation of *SMN*^{tel} loss is very rare, the regulation of gene expression of the centromeric *SMN* could have influence on the disease. This corresponds to the enormous variability in disease severity (1, 5, 8) and suggests that, in the small minority of asymptomatic cases with homozygous *SMN*^{tel} deletion (16, 17, 20, 21), expression of the centromeric copy may fully compensate for loss of the telomeric gene. Indeed, an association of an increased copy number of the centromeric gene with milder forms of SMA has been observed in a recent study (17). Moreover, homozygous deletion of both genes has not been observed in humans (10, 17, 19). To investigate whether *SMN* gene dose has an effect on postnatal motoneuron survival in mice, we have quantitated motoneurons in the facial nucleus of 5-month-old *SMN*$^{+/+}$ and *SMN*$^{+/-}$ mice. In *SMN*$^{+/+}$ mice, 2,394 ± 65 (mean ± SEM, $n = 5$) motoneurons were counted; in *SMN*$^{+/-}$ mice 2,486 ± 253 (mean ± SEM, $n = 4$) motoneurons were counted. The difference was not statistically significant ($P > 0.05$, Student's t test), indicating that a 50% reduction of gene dosage for *SMN* in mice does not lead to degeneration of motoneurons.

The clinical appearance of human spinal muscular atrophy could be explained by the presence and expression of the centromeric copy in human. Thus, the telomeric *SMN* gene defect may cause cell death and dysfunction in SMA patients only in such cells where the centromeric copy is not expressed in sufficient quantities, most probably in motor neurons.

A recent study has identified the SMN protein as a constituent of nucleosomal structures (23). Using the yeast two-hybrid system, SMN has been found to associate with the RGG box of heterogeneous nuclear ribonucleoprotein U and fibrillarin. Additional immunohistochemical evidence suggests that it is localized in specific nucleosomes called gems that are associated with coiled bodies (23). The function of these nucleosomal structures is not clear, but it is attractive to speculate that they are involved in the complex mechanism of nuclear RNA processing (23). The massive cell death detectable in *SMN*-deficient mouse embryos is indeed compatible with such an essential cellular function of the *SMN* gene product.

We thank Timo Grimm, Matthew Digby, and Judith Melki for helpful discussions; Thomas Boehm for the gift of the λPS library; Bettina Holtmann for help with the embryo analysis; Boris Böddinghaus for help with the *lacZ* stain and providing RNA samples. We also thank Michaela Lederer and Michaela Pfister for technical assistance generating sequence data, and Helga Brünner, Bianca Hagemann, Luise Anderson, and Vanessa McGilliard for mouse husbandry. This work was supported by the Deutsche Forschungsgemeinschaft (Klinische Forschergruppe Neuroregeneration, To 61/8–1) and the Biotechnology and Biological Sciences Research Council (United Kingdom).

1. Dubowitz, V. (1995) *Muscle Disorders in Childhood* (Saunders, London), pp. 325–369.
2. Pearn, J. H. (1980) *Lancet* **i,** 919–922.
3. Crawford, T. O. (1996) *Neurology* **46,** 335–340.
4. Munsat, T. L. (1991) *Neuromuscular Disorders* **1,** 81.
5. Zerres, K. & Rudnik-Schöneborn, S. (1995) *Arch. Neurol.* **52,** 518–523.
6. Brzustowicz, L. M., Lehner, T., Castilla, L. H., Penchaszadeh, G. K., Wilhelmsen, K. C., Daniels, R., Davies, K. E., Leppert, M., Ziter, F., Wood, D., Dubowitz, V., Zerres, K., Hausmanowa-Petrusewicz, I., Ott, J., Munsat, T. L. & Gilliam, T. C. (1990) *Nature (London)* **344,** 540–541.
7. Melki, J., Abdelhak, S., Sheth, P., Bachelot, M. F., Burlet, P., *et al.* (1990) *Nature (London)* **344,** 767–768.
8. Gilliam, T. C., Brzustowicz, L. M., Castilla, L. H., Lehner, T., Penchaszadeh, G. K., Daniels, R. J., Byth, B. C., Knowles, J., Hislop, J. E., Shapira, Y., Dubowitz, V., Munsat, T. L., Ott, J. & Davies, K. E. (1990) *Nature (London)* **345,** 823–825.
9. Melki, J., Sheth, P., Abdelhak, S., Burlet, P., Bachelot, M. F., Lathrop, M., Frézal, J., Munnich, A. & the French Spinal Muscular Atrophy Investigators (1990) *Lancet* **336,** 271–273.
10. Lefebvre, S., Burglen, L., Reboullet, S., Clermont, O., Burlet, P., Viollet, L., Benichou, B., Cruaud, C., Millasseau, P., Zeviani, M., Le Paslier, D., Frézal, J., Cohen, D., Weissenbach, J., Munnich, A. & Melki, J. (1995) *Cell* **80,** 155–165.

11. Roy, N., Mahadevan, M. S., Mclean, M., Shutler, G., Yaraghi, Z., Farahani, R., Baird, S., Besner-Johnson, A., Lefebvre, C., Kang, X., Salih, M., Aubry, H., Tamai, K., Guan, X., Ioannou, P., Crawford, T. O., de Jong, P., Surh, L., Ikeda, J., Korneluk, R. G. & Mackenzie, A. (1995) *Cell* **80,** 167–178.
12. Thompson, T. G., DiDonato, C. J., Simard, L. R., Ingraham, S. E., Burghes, A. H. M., Crawford, T. O., Rochette, C., Mendell, J. R. & Wasmuth, J. J. (1995) *Nat. Genet.* **9,** 56–62.
13. Mahadevan, M. S., Korneluk, R. G., Roy, N., MacKenzie, A. & Ikeda, J.-E (1995) *Nat. Genet.* **9,** 112–113.
14. Lewin, B. (1995) *Cell* **80,** 1–5.
15. Liston, P., Roy, N., Tamai, K., Lefebvre, C., Baird, S., Cherton-Horvat, G., Farahani, R., McLean, M., Ikeda, J., MacKenzie, A. & Korneluk, R. (1996) *Nature (London)* **375,** 349–353.
16. Cobben, J. M., van der Steege, G., Grootscholten, P., de Visser, M., Scheffer, H. & Buys, C. H. C. M. (1995) *Am. J. Hum. Genet.* **57,** 805–808.
17. Velasco, E., Valero, C., Valero, A., Moreno, F. & Hernández-Chico, C. (1996) *Hum. Mol. Genet.* **5,** 257–263.
18. Capon, F., Levato, C., Semprini, S., Pizzuti, A., Merlini, L., Novelli, G. & Dallapiccola, B. (1996) *Muscle Nerve* **19,** 378–380.
19. Rodrigues, N. R., Owen, N., Talbot, K., Ignatius, J., Dubowitz, V. & Davies, K. E. (1995) *Hum. Mol. Genet.* **4,** 631–634.
20. Hahnen, E., Forkert, R., Marke, C., Rudnik-Schöneborn, S., Schonling, J., Zerres, K. & Wirth, B. (1995) *Hum. Mol. Genet.* **4,** 1927–1933.
21. Wang, C. H., Xu, J., Carter, T., Ross, B. M., Dorniniski, M. K., Bellcross, C. A., Penchaszadeh, G. K., Munsat, T. L. & Gilliam, T. C. (1996) *Hum. Mol. Genet.* **5,** 359–365.
22. Bussaglia, E., Clermont, O., Tizzano, E., Lefebvre, S., Bürglen, L., Cruaud, C., Urtizberea, J. A., Colomer, J., Munnich, A., Baiget, M. & Melki, J. (1995) *Nat. Genet.* **11,** 335–337.
23. Liu, Q. & Dreyfuss, G. (1996) *EMBO J.* **15,** 3555–3565.
24. Nehls, M., Messerle, M., Sirulnik, A., Smith, A. J. & Boehm, T. (1994) *BioTechniques* **17,** 770–775.
25. Le Mouellic, H., Lallemand, Y. & Brület, P. (1990) *Proc. Natl. Acad. Sci. USA* **87,** 4712–4716.
26. Smith, A. G. (1991) *J. Tissue Culture Methods* **13,** 89–94.
27. Vernet, M., Bonnerot, C., Brian, P. & Nicolas, J.-F. (1993) *Methods Enzymol.* **225,** 434–451.
28. Sambrook, J., Fritsch, E. F. & Maniatis, T. (1989) *Molecular Cloning: A Laboratory Manual* (Cold Spring Harbor Lab. Press, Plainview, NY).
29. Sanes, J., Rubenstein, J. R. L. & Nicolas, J.-F. (1986) *EMBO J.* **5,** 3133–3142.
30. Masu, Y., Wolf, E., Holtmann, B., Sendtner, M., Brem, G. & Thoenen, H. (1993) *Nature (London)* **365,** 27–32.
31. Schuler, G. D., Altschul, S. F. & Lipman, D. J. (1991) *Proteins* **9,** 180–190.
32. Gennarelli, M., Lucarelli, M., Capon, F., Pizzuti, A., Merlini, L., Angelini, C., Novelli, G. & Dallapiccola, B. (1995) *Biochem. Biophys. Res. Commun.* **213,** 342–348.
33. Hogan, B., Beddington, R., Costantini, F. & Lacy, E. (1994) *Manipulating the Mouse Embryo* (Cold Spring Harbor Lab. Press, Plainview, NY), pp. 41–56.
34. El-Shershaby, A. M. & Hinchcliffe, J. R. (1974) *J. Embryol. Exp. Morphol.* **31,** 643–654.